ASTROBIOLOGY
Volume 4, Number 1, 2004

Research Paper

Hydrogen Emission in Meteors as a Potential Marker for the Exogenous Delivery of Organics and Water

PETER JENNISKENS[1] and AVRAM M. MANDELL[2,*]

ABSTRACT

We detected hydrogen Balmer-alpha (H_α) emission in the spectra of bright meteors and investigated its potential use as a tracer for exogenous delivery of organic matter. We found that it is critical to observe the meteors with high enough spatial resolution to distinguish the 656.46 nm H_α emission from the 657.46 nm intercombination line of neutral calcium, which was bright in the meteor afterglow. The H_α line peak stayed in constant ratio to the atmospheric emissions of nitrogen during descent of the meteoroid. If all of the hydrogen originates in the Earth's atmosphere, the hydrogen atoms are expected to have been excited at T = 4,400 K. In that case, we measured an H_2O abundance in excess of 150 ± 20 ppm at 80–90 km altitude (assuming local thermodynamic equilibrium in the air plasma). This compares with an expected <20 ppm from H_2O in the gas phase. Alternatively, meteoric refractory organic matter (and water bound in meteoroid minerals) could have caused the observed H_α emission, but only if the line is excited in a hot T ~10,000 K plasma component that is unique to meteoric ablation vapor emissions such as Si^+. Assuming that the Si^+ lines of the Leonid spectrum would need the same hot excitation conditions, and a typical [H]/[C] = 1 in cometary refractory organics, we calculated an abundance ratio [C]/[Si] = 3.9 ± 1.4 for the dust of comet 55P/Tempel-Tuttle. This range agreed with the value of [C]/[Si] = 4.4 measured for comet 1P/Halley dust. Unless there is 10 times more water vapor in the upper atmosphere than expected, we conclude that a significant fraction of the hydrogen atoms in the observed meteor plasma originated in the meteoroid. Key Words: Prebiotic molecules—Origin of life—Meteors—Molecular band emission. Astrobiology 4, 123–134.

INTRODUCTION

ATOMIC HYDROGEN EMISSION may be the only readily observable signature of organic matter in meteors during exogenous delivery. Meteors represent a unique chemical pathway towards prebiotic compounds on the early Earth (Jenniskens *et al.*, 2000a, 2004a,b). Other pathways from cometary and asteroidal organics to prebiotic compounds include giant impacts during the final stages of planet accretion, and the steady rain of interplanetary dust particles and micro-

[1]Center for the Study of Life in the Universe, SETI Institute, Mountain View, California.
[2]NASA Ames Astrobiology Academy, NASA Ames Research Center, Moffett Field, California.
*Present address: Astronomy and Astrophysics Department, The Pennsylvania State University, State College, Pennsylvania.

meteorites that survived passage through Earth's atmosphere (Oró, 1961; Chyba and Sagan, 1992, 1997; Delsemme, 1992; Brack, 1999; Maurette *et al.*, 2000). Meteors are significant because the bulk of infalling meteoroid mass is ablated in Earth's atmosphere.

A significant fraction, if not all, of the refractory organic matter is expected to remain in the meteoroids after ejection from a comet, acting as a glue that holds the silicate grains together. An open question is how much organics are still there at the time of impact with Earth.

During ablation, meteoric organic matter can undergo unique chemical processes in the heated meteoroid and in the rarefied high Mach number flow of the meteor plasma, the physical conditions of which are studied by remote sensing of present-day meteors (Jenniskens *et al.*, 2000a). Organic matter can lose hydrogen atoms if the material is completely dissociated, or in a process called carbonization, which is the loss of functional groups and simultaneous growth of the carbon skeleton, a process commonly observed when organic matter is exposed to energetic particles and ultraviolet light (Jenniskens *et al.*, 1993).

We conducted high-resolution spectroscopic studies of meteors at visible wavelengths during the recent November 18, 2001, Leonid storm, onboard the NASA and U.S. Air Force-sponsored Leonid Multi-Instrument Aircraft Campaign (Leonid MAC) (Jenniskens and Russell, 2003). Highest rates were observed at 10:40 universal time (UT), when Earth crossed the dust ejected from comet 55P/Tempel-Tuttle during its return in 1767 (Kondrat'eva and Reznikov, 1985).

Elsewhere in this issue we focused on the search for the CN radical, a small diatomic organic breakup product, and found much less CN than expected if the meteoric organic matter is efficiently decomposed (Jenniskens *et al.*, 2004a). If, on the other hand, the organic matter is carbonized by a loss of functional groups such as -OH and -H (Jenniskens and Stenbaek-Nielsen, 2004), then CN radicals would be rare but hydrogen atoms might be detected.

Hydrogen may also originate from water and hydrogen-containing minerals in the meteoroid. At the typical $T \sim$4,400 K temperatures in meteor plasma (Jenniskens *et al.*, 2004b), water molecules and OH radicals are quickly dissociated, producing hydrogen atoms. The water in our oceans may have been delivered by meteoroids if they contained significant amounts of water with a D/H ratio more similar to that of our ocean than comet ice (Maurette *et al.*, 2000). Cometary meteoroids are thought to lose much, if not all, of their icy volatiles to the vacuum of space after release (Lellouch *et al.*, 1998). It is not known if they contain water bound to minerals (see discussion in Jenniskens *et al.*, 2004c). On the other hand, OH *A-X* (0,0) emission at 310 nm has previously been identified in meteor spectra, including those of Leonids (Harvey, 1977; Abe *et al.*, 2002; Jenniskens *et al.*, 2002). We did not find ground-state OH $X^2\Pi$ Meinel band emission in Leonid spectra, providing support to the hypothesis that the OH originates from the dissociation of water (Jenniskens *et al.*, 2004c).

This suggested to us to look for hydrogen emission in meteors. Unfortunately, the strongest optical line of the hydrogen Balmer series, hydrogen Balmer-alpha (H_α), has a high excitation energy of 12.09 eV and is expected to be weak if thermally excited at 4,400 K. However, it has been hypothesized that a hot $T \sim$10,000 K component exists in meteor plasma, which is responsible for the strong Ca^+ and Si^+ lines seen in bright and fast meteors (Borovicka, 1994a). This component would provide sufficient population of the upper state for the H_α line to become visible for the expected abundances.

Indeed, Borovička and Jenniskens (2000) reported the detection of H_α emission from low-resolution spectra of the −13 magnitude "Y2K" Leonid fireball observed during the 1999 Leonid MAC mission, and derived an abundance ratio of [H]/[Fe] = 10–20. The hydrogen line was identified only in the meteor spectrum itself, not in the meteor afterglow. Before that, several other authors reported H_α in low-resolution spectra (*e.g.*, Cook and Millman, 1955) or in relatively confused high-resolution spectra of bright fireballs (*e.g.*, Ceplecha, 1971). These identifications are sometimes in doubt, and the hydrogen abundance was not quantified. H_α was not detected in the high-quality ($\Delta\lambda$ = 0.7 nm) photographic spectrum of the slow −9th magnitude fireball EN 151068 (Borovička, 1994b).

Whether hydrogen is present in meteor spectra needs to be established before addressing the question how much hydrogen derives from the meteoroid (from organics or water) or from the ambient atmosphere.

METHODS

Until now, the success rate of capturing good-quality meteor spectra with traditional photographic techniques has been low, typically only one good spectrum per year per camera (Millman, 1980). The photographic cameras in use need a rare very bright fireball (−5 magnitude or brighter) to provide a good spectrum. Key to increasing the sensitivity to more common fainter meteors, and still maintaining a high spectral resolution, is to use cooled charge coupled device (CCD) cameras. Cooled CCD cameras are about 5 magnitudes more sensitive than photographic plates. The instrumental layout and response functions of our two-stage thermoelectrically cooled slit-less CCD spectrograph is discussed elsewhere in this issue (Jenniskens *et al.,* 2004a). By purposely limiting the spectral range to about 100 nm over the 1,024 × 1,024 pixel CCD range, a spectral resolution is obtained of $\Delta\lambda = 0.54$ nm in first order, which is similar to, or better than, that of traditional photographic slit-less spectrographs.

RESULTS

The observation of meteor storms further increases the detection rate. During the November 2001 Leonid storm, the instrument was deployed behind an optically flat BK7-type glass window onboard the U.S. Air Force/418th Flight Test Squadron-operated NKC-135 "FISTA" research aircraft from an elevation of 37,000 ft. This was a single-plane mission en route from Alabama to California, supported by ground stations in Arizona (Jenniskens and Russell, 2003). Additional spectra were obtained during a ground-based observing run at Fremont Peak Observatory in California at the time of the December 12 and 13, 2001, Geminid shower.

At 10:52:32 UT (November 18, 2001), a particularly strong emission line close to the expected H_α line was detected in the spectrum of a −8 magnitude Leonid fireball, known by the data analyzers as "Ha!," after it was recognized that H_α emission was present. This was the brightest meteor detected with this instrument during that mission. The "Ha!" fireball was recorded too by a low-resolution intensified video camera (Fig. 1). After a gradual brightening, a strong flare was observed, and a small fragment continued to lower altitudes in a pattern that was similar to the well-documented "Y2K" fireball (Borovička and Jenniskens, 2000; Jenniskens and Rairden, 2000). A persistent train was seen for 12 min. The meteor appeared in the constellation Draco and peaked at an elevation of 21° above the horizon, 10° east from north, when the plane was at the coordinates 108.04 W, 35.00 N, south of Gallup, NM. Unfortunately, this was just out of reach of our ground stations in Arizona, and no trajectory data are available. From the altitude of the "Y2K" persistent train (92–79 km, with a peak at 84 km), we surmise that the "Ha!" meteor peaked also at or just above 84 km, and penetrated to an altitude between 79 and 84 km.

The first order spectrum is shown in Fig. 2. Just after the sodium line intensity peaked, there was

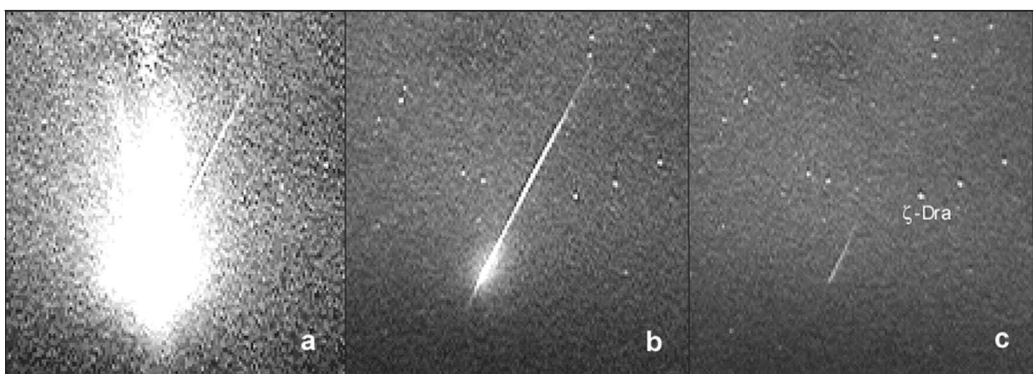

FIG. 1. The 10:52:32 UT Leonid meteor as recorded by an intensified video camera. The field of view is about 15 × 15°. From left to right: (**a**) the meteor at its peak brightness ($t = 0$ s); (**b**) the afterglow (bottom) and the 557 nm O I wake (top) immediately following the meteor in an average of four frames ($t = 0.16$ s); and (**c**) the persistent train 6 s after the meteor, in an average of 8 frames.

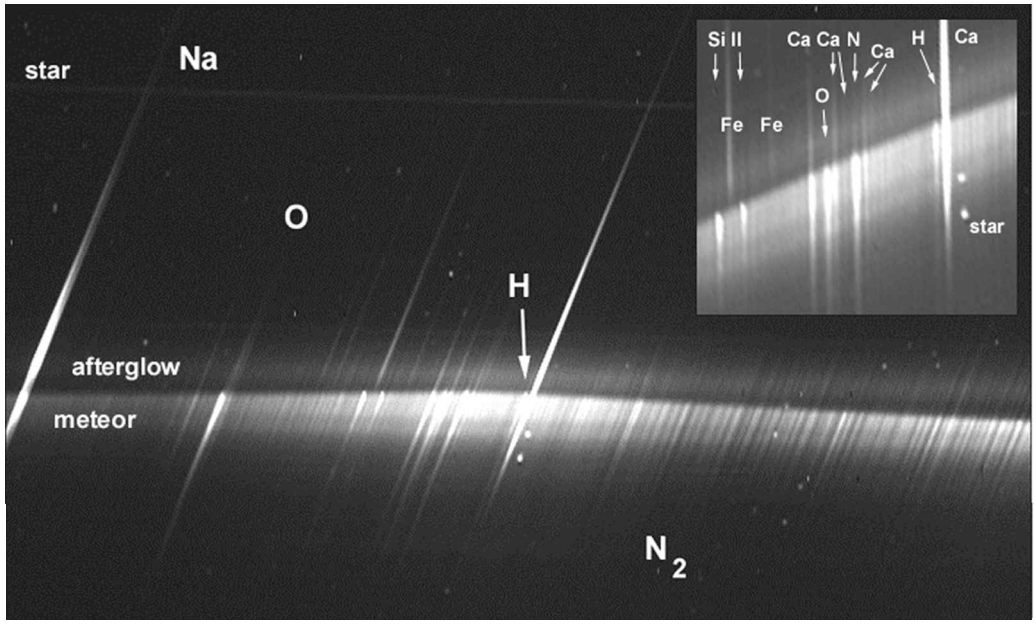

FIG. 2. First order spectrum of the 10:52:32 UT "Ha!" Leonid meteor in the range 588–720 nm. The spectrum has been expanded by a factor of 4 in vertical direction to undo the effect of binning, and the image is shown reversed, so that the wavelength scale runs left to right. The meteor moved from top to bottom. The main atomic lines and bands are identified. **Inset:** An enlargement of the center part of the spectrum, showing the hydrogen emission in the afterglow and along the length of the meteor spectrum.

an abrupt change of the spectrum, and high excitation lines appeared. This was the position of the meteoroid when the camera shutter opened and the meteor itself came in view. At positions where the meteoroid was prior to this point, the recorded spectrum was that of the meteor afterglow (top part of Fig. 2). Although afterglow and meteor were integrated for 0.800 s, the afterglow at positions earlier along the trajectory had decayed more than positions closer to the meteoroid at the start of the exposure. The integration time was not long enough to detect any chemiluminescence from a persistent train. At positions where the meteoroid was seen while the shutter was open, the spectrum is dominated by the meteor itself, which persists for ~0.02 s, with a minor contribution from the afterglow, significant only in the sodium lines and the strong intercombination line of Ca I at 657 nm. The onset of the meteor exposure was slightly earlier at the center of the plate because the meteoroid was in motion, while the shutter opened starting from the center. There were periodic variations in the light intensity along the trajectory, most likely due to a modulation of vapor production with the rotation of the meteoroid at a rate of about 46 cycles/s.

The spectrum of meteor and afterglow are different, as described in detail for the "Y2K" Leonid fireball in Borovička and Jenniskens (2000). In short, the meteor spectrum consists predominantly of allowed transitions of atoms and ions of both low excitation (*e.g.,* lines of Na I, Fe I, Ca II) and high excitation (*e.g.,* O I, N I, H I, Si II). The afterglow only has low excitation lines, but this includes also excitation lines with low transition probability (*e.g.,* Ca I at 657 nm, Fe I at 636 nm, and many others), which are very faint in the spectrum of the fireball itself.

The late start of the exposure was fortunate. It enabled the separation of the fireball and afterglow spectrum. This is normally possible only for video spectra (low resolution) and photographic spectra with a rotating shutter. Moreover, the fireball spectrum would have been heavily overexposed at the position of the flare.

Line identification

Because of the small detector size, the wavelength scale is almost linear, and wavelength calibrations can be performed by matching known lines in the spectrum. Lines were identified by calibrating the vacuum wavelength of the sodium

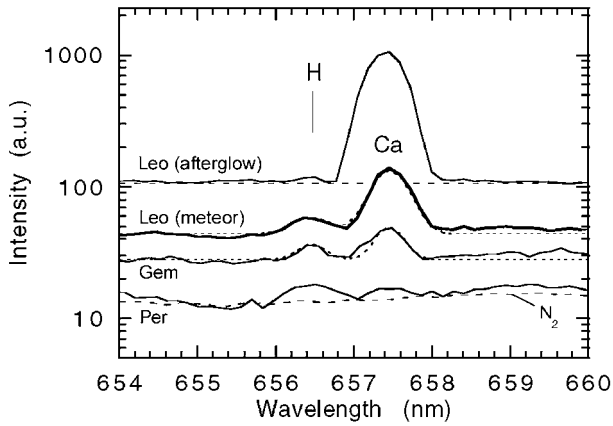

FIG. 3. Extracted H_α and calcium emission lines. Shown are average Leonid spectra from afterglow and meteor. The comparison spectra are the Geminid and Perseid meteors discussed in the text. Dashed lines depict the background emission from molecular nitrogen. Dotted lines in the middle two spectra are the fitted line profiles for H and Ca emission, respectively, which are based on the line positions and the instrumental line profile, and are matched to fit the observed peak intensity of the lines.

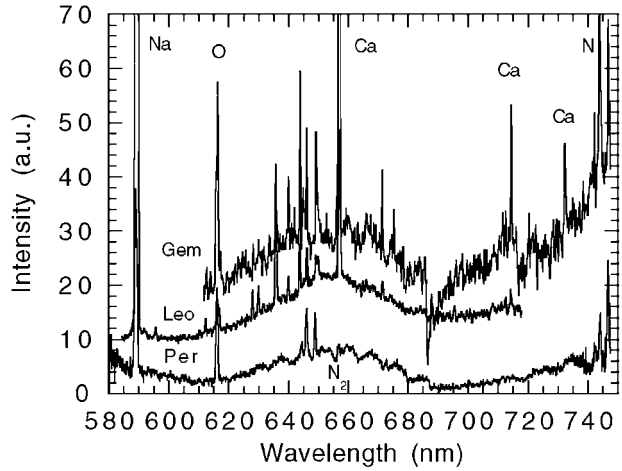

FIG. 5. Comparison of the Leonid, Geminid, and Perseid meteor spectra. Leonid and Geminid spectra are displaced upward to facilitate comparison. Note the strong telluric absorption of oxygen and water in the ground-based spectrum of the Geminid. Also note the absence of metal atom ablation in the fainter Perseid.

doublet to the theoretical wavelength scale (Jenniskens *et al.,* 2004a). Any Doppler shift from residual meteor motion is negligibly small and systematic. Subsequently, all of the emissions expected from neutral metal atoms and singly ionized elements were matched to the observed line positions. For the first order, there is no order overlap below about 740 nm due to a fast drop of optical transmittance below 370 nm.

We found that many strong emission lines in this wavelength range are due to neutral calcium. With that information in hand, many other lines were also identified (Table 1). The wavelength

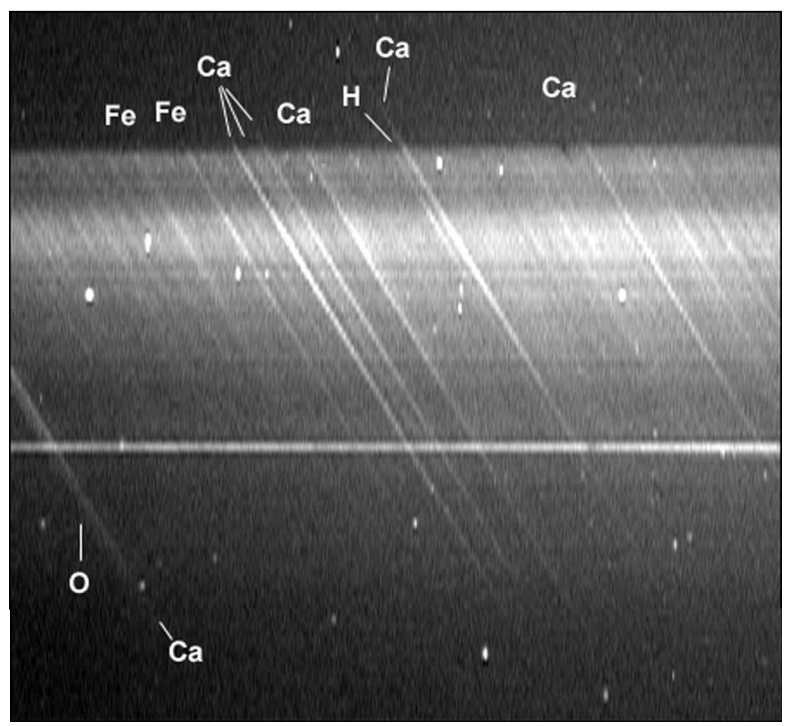

FIG. 4. Hydrogen emission in the Geminid of 07:15:28 UT (December 14, 2001), from a ground-based observation from Fremont Peak Observatory in California. The horizontal line is a star spectrum, and dots are first order star images.

TABLE 1. LINE IDENTIFICATIONS

Wavelength			∑ intensity		
Observed	*Theory, vacuum*	*Element*	*Leonid, afterglow*	*Leonid, meteor*	*Geminid, meteor*
589.09	589.1584	Na I (D)	1,036	—	—
589.67	589.7558	Na I (D)	671	—	—
591.93	591.5753	Fe I, low E?	5	—	—
595.88	595.8342	Fe I, low E	12	—	—
610.47	610.4412	Ca I	6	3	4.8
612.51	612.3912	Ca I	15	9	5.8
613.82	613.8313	Fe I	2	<2	4.8
614.08	613.9393	Fe I	4	3	4.0
615.99	615.7675/615.8459/615.9876	O I	<7	86	17
616.46	616.3878/x.3001/x.5462/x.8146	Ca I	32	16	40
617.12	617.0750/617.1272	Ca I	21	11	4.6
617.58	617.5049	Fe I	<2	<2	2.3
619.09	619.3271	Fe I	<2	<2	4.2
622.36	622.3391	Fe I, low E	<2	<2	1.5
623.25	623.2450	Fe I	<2	<2	3.5
623.72	—	Unidentified	4	<2	2.3
624.67	624.8045	Fe I	<3	<2	2.9
625.58	625.4284	Fe I	<2	<2	2.9
628.31	628.2353	Fe I, low E	24	<2	3.7
630.28	630.3241/630.4237	Fe I	21	<2	4.3
632.01	631.7052/9765/2.4438 (1.9856)	Fe I (Ca I)	2	5	2.6
633.86	633.7080/633.8575	Fe I	<2	<2	19
634.99	634.8849	Si II	<2	14	<1
635.66	635.5592	Fe I, low E	—	<2	3.5
636.12	636.0451	Fe I, low E	117	0	7.8
636.30	636.3545	Ca I	—	<2	3.5
637.36	637.3125	Si II	3	7	<2
638.34	—	Unidentified	6	<2	1.7
638.71	—	Unidentified	6	<2	<2
640.30	640.2083	Fe I, low E	18	<2	12
641.27	640.9787/641.3419	Fe I	2	<2	3.2
642.18	642.3124	Fe I	<2	<2	2.6
644.06	644.0855	Ca I	28	20	32
644.28	644.2718	N I	2	10	—
645.25	645.1592	Ca I	10	8	9.5
645.79	645.77/645.62/645.53	O I	<5	43	6.9
646.52	646.4351	Ca I	30	18	20
647.38	647.3450	Ca I	7	4	2.9
648.57	648.6600/648.4490/648.5545	N I	6	42	<2
649.55	649.5576	Ca I	19	8	20
650.20	650.0733	Fe I, low E	17	<2	9.0
652.97	—	Unidentified	<2	<2	3.5
654.59	654.9381	Fe I, low E	<2	<2	1.5
656.53	**656.4636**	**H I**	**6**	**15**	**9.0**
657.57	657.4595	Ca I	760	90[a]	20
659.55	659.4734/659.5692	Fe I	<2	<2	2.3
661.15	661.1502	Fe I, low E	<2	<3	2.0
671.94	671.9536	Ca I	11	10	14
672.60	672.4466/672.5309	N I	7	12	1.0
715.12	715.0120	Ca I	15	15	23
732.77	732.8163	Ca I	—	—	17
742.50	742.5686	N I	—	—	14
744.33	744.4348	N I	—	—	40
747.00	747.0369	N I	—	—	36

These are vacuum wavelengths. Integrated line intensities are in arbitrary units after correction for instrument response. The line in boldface type is the H_α line discussed in the text.

[a]Contaminated by afterglow.

scale is accurate to about half a pixel: ±0.07 nm. At the altitude of the observations (37,000 ft) there was no detectable atmospheric water vapor absorption. Many of the weaker features seen in the spectrum are due to vibrational and rotational structure in the underlying First Positive band of N_2.

We found that the expected position of H_α (656.46 nm) did not align with the brightest emission line, identified as the intercombination 657.46 nm line of calcium (Poole, 1979), but with a fainter emission line just next to it. Figure 3 shows the line profiles from row averages at positions where the meteor was before and after opening of the shutter. The dashed line shows the line positions of H_α and Ca I, convolved with the instrumental line profile. A good match is obtained after scaling the line intensities to match the observed lines. The line intensity ratio H/Ca equalled 0.17.

Corroborating evidence for the presence of both H_α and the Ca I line comes from the spectrum of an intrinsically slower Geminid (36.3 ± 0.6 km/s rather than 71.6 ± 0.4 km/s) shown in Fig. 4. A comparison of the details of the raw data near the H_α line in Figs. 3 and 4 reveal many similarities. Though the meteor was not observed in a wide-field imager, it must have been located near the horizon judging from the presence of the strong telluric oxygen O_2 *B*-band (686–688 nm) absorption in this spectrum (Fig. 5). The integrated intensity over the final part of the Geminid spectrum is about 1.1 magnitude fainter than that for the Leonid fireball. The line intensity ratio H/Ca equalled 0.41 (Fig. 3).

The Geminid spectrum is rich in metal atom emission lines. Air plasma emissions were also detected. The exposure was started before the meteor's peak brightness. At positions just before the position of the meteor at the onset of exposure (upper part of Fig. 3), afterglow emission was observed. Geminids are not known to have flares like the Leonids, but some more-rapid-than-expected variations of the light curve can be recognized shortly after the beginning of the exposure. The Geminid produced a repetitive series of dark bands that are less well separated than in the "Ha!" meteor, indicative of rotation of the meteoroid at a rate of about 40 cycles/s.

No such calcium or hydrogen emission was observed in a fainter −3 magnitude Perseid meteor observed at 10:35:26 UT (August 13, 1999) as shown in Fig. 5 (Jenniskens *et al.*, 2000a). The Perseid meteor was detected, too, by a second camera and appeared high in the sky. As expected, it has less telluric O_2 *B*-band absorption. The spectrum has a lower spectral resolution due to a less favorable orientation of the meteor trajectory relative to the dispersion direction of the grating. Because of the much weaker metal atom ablation lines, this spectrum illustrates the thermal emissions from oxygen and nitrogen atoms. Note that this spectrum, too, has an H_α line as strong as that in the Leonid and Geminid spectra, as well as a faint calcium intercombination line, with intensity ratio H/Ca equal to 0.69 (Fig. 3).

Temporal variation

The temporal variation of various representative emission lines in the "Ha!" Leonid is shown in Fig. 6. In the afterglow phase, neutral metal atoms of sodium, iron, and calcium, which derive from widely varying volatile minerals but have similar excitation energies, follow initially the same exponential increase in intensity. Sodium remains in the same proportion to iron and calcium during the afterglow, implying that there was no differential ablation in this part of the trajectory. Minerals containing sodium did not ablate earlier than the less volatile minerals containing calcium. The light curve reflects the exponential increase in brightness of the meteor, leading up to a flare that occurred just before opening of the shutter.

The "Ha!" meteor's spectrum is dominated by air plasma emissions from nitrogen molecules and atoms, but metal atom ablation lines are also observed (Table 1). Low excitation lines of iron ($E_i < 4$ eV) are comparatively weak, but calcium and sodium lines are stronger than in the afterglow earlier in the trajectory. This suggests that a significant part of the calcium emission is from the meteor phase. For T = 4,400 K, we calculated an abundance ratio of [Ca]/[Fe] equal to 0.13. In good agreement with this finding is the result of Rietmeijer and Nuth (2000), who calculated that comet 1P/Halley's dust has a [Ca]/[Fe] ratio of 0.12. Hence, in this particular meteor, the calcium was ablated as efficiently as iron. The decrease of light from the strong sodium and calcium lines is exponential and follows the same slope as the air plasma emissions, reflecting a weakening of the meteor after the earlier flare. The ionized silicon emission has an interesting flare at row 15 (Fig. 7) that was not seen in other lines, including the

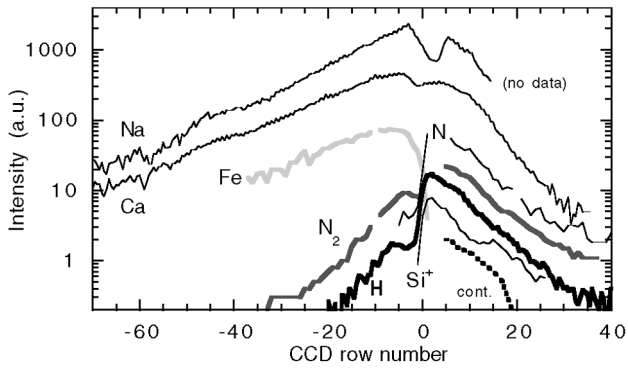

FIG. 6. Light curves for representative emission lines and bands. The bold line is the light curve of neutral hydrogen atomic emission (H I, 656.53 nm). Metal atom emissions are: neutral sodium (Na I, 595 + 589 nm), neutral calcium (Ca I, 657 nm), neutral iron (Fe I, 636 nm), and ionized silicon (Si^+, 635 + 637 nm). The lines of nitrogen atoms (N, 649 nm) and nitrogen molecules (N_2) trace the air plasma components. "cont" refers to a continuum component. Row numbers less than zero trace the afterglow emissions behind the meteor. Row number 0 corresponds to the start of the exposure. The shift in the onset of meteor sodium emission, found at the edge of the spectrum, is due to the gradual opening of the camera shutter.

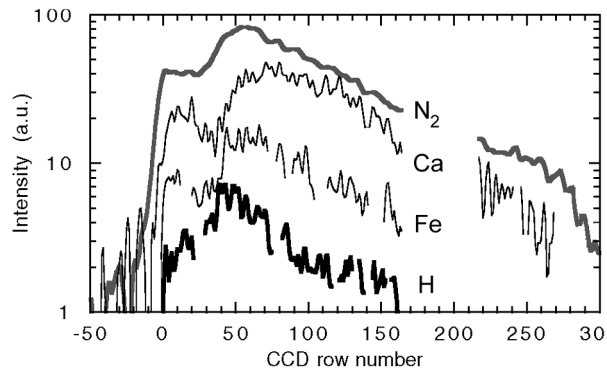

FIG. 7. As Fig. 6, for the Geminid spectrum of Fig. 4. Note how the Ca I 657 nm line peaks later than other emissions.

nitrogen and oxygen lines, except (more weakly) in the hydrogen line.

Compared with sodium and calcium, the emission intensity of atmospheric N_2 decreased more rapidly behind the meteor, in the same rapid manner as hydrogen. Both emissions have relatively high excitation energies, and the rapid decrease is on account of that. In previous work, we calculated the temperature decline behind the meteoroid from this rate of decay (Borovička and Jenniskens, 2000; Jenniskens and Stenbaek-Nielsen, 2004).

Judging from the increased ratio of N I/N_2 emission (Jenniskens *et al.*, 2004b), the plasma was slightly warmer in the meteor than in the afterglow, as expected (Borovička and Jenniskens, 2000). At this time, there was a detectable continuum emission, possibly because of dust or N_2^+ emission (Jenniskens *et al.*, 2004c). Fitting the observed spectrum with a model air plasma spectrum as in Jenniskens *et al.* (2004b,c) provided a means to separate the continuum and N_2 band. The band intensity at the center of the image is uncertain because of what appears to be a reflection of light in the window with a Gaussian distribution peaking at the center of the CCD.

The ratio of N I/N_2 is lower in the slower Geminid than in the Leonid, corresponding to an equivalent local thermodynamic equilibrium air plasma temperature of $T = 4{,}355$ K, versus $T = 4{,}470$ K for the Leonid.

The lower plasma temperature in the afterglow would correspond to a relatively higher N_2 abundance if chemical equilibrium is maintained. Indeed, the ratio of H_α/N_2 line intensities was higher in the meteor (Fig. 6). The H_α line in the meteor spectrum also falls off less steeply than the Ca I 657 nm emission, with a light curve more similar to the N_2 air plasma emission. In the same way, the H_α line in the Geminid spectrum follows the broadband emission from molecular nitrogen, rather than the meteoric calcium intercombination line, which has a broad maximum that peaks slightly later than the air plasma emission (Fig. 7).

From these results we calculated the abundances of hydrogen atoms in the Leonid meteor plasma and in the afterglow, following the method by Borovička (1993). In the meteor plasma, where nitrogen and oxygen atom emissions are best defined, we calculate that $[H]/[N] = 1.1 \pm 0.3 \times 10^{-2}$ and $[O]/[N] = 3.0 \pm 0.3$ (for the Geminid meteor), assuming that all emission originates from a $T = 4{,}400$ K plasma. The latter value differs from the expected value of 0.25, if similar amounts of oxygen and nitrogen molecules were dissociated in the meteor plasma. This suggests that less molecular nitrogen is dissociated than expected. If all oxygen molecules are dissociated, then that $[H]/[N] = 9.2 \pm 1.7 \times 10^{-4}$. In another Leonid meteor, the fraction of dissociated molecular oxygen was measured to be as low as 15% (Jenniskens *et al.*, 2000b), or $[H]/[N] = 1.4 \pm 0.3 \times 10^{-4}$. Here, N is the total amount of

nitrogen atoms in the plasma in atomic and molecular form. Because the observed transitions of hydrogen, oxygen, and nitrogen atoms have about the same upper energy level, these results are insensitive to the adopted plasma temperature.

DISCUSSION

Atmospheric sources of hydrogen

Let us first consider the possibility that the hydrogen is due to water vapor in the ambient atmosphere. At the meteor plasma temperature of 4,400 K, water is effectively dissociated into H and OH, and, given sufficient time, OH is dissociated into O and H (Fig. 8 in Jenniskens *et al.,* 2004c). From the $[H]/[N] = 1.4 \pm 0.3 \times 10^{-4}$ result in the previous section, and after taking into account that ~79.8 % of all ambient atmospheric compounds are in the form of molecular nitrogen (with ~19.6% oxygen molecules and ~0.6% oxygen atoms), we calculated that if all hydrogen was due to ambient water (with two hydrogen atoms per molecule), the abundance of water in all forms in the mesopause at the altitude of the meteor (~80–90 km) would be in excess of 165 ppm.

However, the water mixing ratio above 80 km is thought to be typically a few ppm and rarely more than 20 ppm (Conway *et al.,* 1999; Stevens *et al.,* 2001). Above 80 km, water molecules are effectively photolysed by ultraviolet photons, resulting in a drop off of water abundance with altitude, which contributes to a sharp decrease in OH and HO_2 abundances. Above 85 km, most HO_2 reacts with oxygen atoms to form OH, and OH molecules react with oxygen atoms to form hydrogen atoms. H_2 is produced from $H + HO_2$, and is destroyed by reactions with oxygen atoms (Harris, 2001). As a result, most hydrogen is present in the form of hydrogen molecules and atoms. The NCAR 1D TIME model (Roble, 1995) predicts H, H_2, and H_2O concentration of 2.8, 6.5, and 1.4 ppm at 80 km, respectively, and 1.3, 5.4, and 0.1 ppm at 90 km, respectively. OH and HO_2 abundances are negligible sources of hydrogen. With two hydrogen atoms, from each H_2 and H_2O molecule, this adds up to a hydrogen atom abundance of 19 and 12 ppm, at 80 and 90 km altitude, respectively. These values are a factor of 8 and 14 lower than observed. After subtracting the contribution from H and H_2, we calculated that if all hydrogen was due to ambient water, the abundance of water in all forms in the mesopause at the altitude of the meteor (~80–90 km) would be in excess of 150 ± 20 ppm.

In order to explain the high 150 ppm water abundance observed in our data, it is possible that solid water in the form of ice particles or hydrates is evaporated and dissociated rapidly during passage of the meteor. At the lower boundary of the mesopause, heavy molecules detected in rocket experiments are thought to be metal atom hydrates. Meteoric smoke molecules such as $NaHCO_3$ are thought to act as nucleation sites for water clusters [$NaHCO_3 \cdot (H_2O)_n$ with $n > 100$] with sizes up to 20 nm (Plane, 2000). When the temperature drops below 150 K, noctilucent clouds are observed to form at around 83 km as a result of ice particle formation. Noctilucent cloud particles can grow to sizes of 50–800 nm. Just above this altitude, where the particles do not grow as large, polar mesosphere summer echoes are observed that can only be explained by the presence of similar but smaller particles. Regarding these smaller particles, which are estimated to be less than 50 nm, their presence and properties are yet to be proven experimentally.

Such continuous production of water molecules in the plasma may, in fact, account for the OH $A \rightarrow X$ emission at 310 nm (Harvey, 1977; Abe *et al.,* 2002; Jenniskens *et al.,* 2002). However, this would imply that much of the hydrogen in the mesopause is not in the form of molecular hydrogen, but rather in the form of hydrates. The problem with this interpretation is the limited number of collisions with hot air compounds that occur in the brief meteor phase. We know of no simulations that study the evaporation of the hydrates in the meteor plasma, but doubt that the process is rapid enough to evaporate the solid grains in the brief ~0.02 s meteor phase.

Meteoric sources of hydrogen

An alternative hypothesis is that the hydrogen emission is related to the destruction of organics or the outgassing of water bound and trapped in minerals. The hydrogen emission cannot originate from the same warm $T = 4{,}400$ K plasma as the weaker iron lines (Table 1), from which we calculated $[H]/[Fe] = 6 \times 10^6$. However, if both Si II and H I in the Leonid meteor are from a hot component, we calculated a reasonable [H]/[Si] = 4 for the "Ha!" meteor. After adopting a

bulk comet Halley abundance ratio of [Fe]/[Si] = 0.28 (Rietmeijer and Nuth, 2000), this translates to a ratio for [H]/[Fe] = 14, in close agreement with the "Y2K" Leonid fireball result. Borovička and Jenniskens (2000) calculated an abundance ratio of [H]/[Fe] = 10 for the "Y2K" meteor.

Although the hot component is hypothesized to be in the range of about 9,000–15,000 K (Borovička, 1994a), no reliable measurement of the temperature of the hot component exists. If the hot component is assumed to be 8,000 K, we calculated [H]/[Fe] = 35, and at 15,000 K the ratio of [H]/[Fe] equals 9. We adopt [H]/[Fe] = 14 ± 5, if all hydrogen in the spectrum of "Ha!" derived from the meteoroid.

The hot component is a small fraction of the total plasma volume. If a volume of such a hot component (V_{Hot}) is responsible for the H I emission, but a volume of iron is collisionally excited by the warm 4,400 K plasma (V_{Warm}), and by assuming and abundance ratio [H]/[Fe] = 14 in both components, we find $V_{\mathrm{Hot}}/V_{\mathrm{Warm}} = 6 \times 10^{-4}$ for this meteor if all hydrogen is meteoric in origin. Such small volume makes it possible that the hot component is related to the impact excitation during the expansion phase at the time when molecules collide with remnant non-thermal speeds. Those collisions involve a larger fraction of metal ablation products than later thermal collisions.

Comet Halley has a ratio of [H]/[C] = 1 in its refractory organic component (Greenberg, 2000), and about equal amounts of refractory organics and silicates. Assuming [H]/[C] = 1, we calculated that [C]/[Si] = 3.9 ± 1.4. This is in good agreement with the ratio of [C]/[Si] = 4.4 measured in the spectrum from bulk comet Halley dust (Rietmeijer and Nuth, 2000). It appears that the meteoroids of comet 55P/Tempel-Tuttle ejected in 1767 are still as rich in organic matter as the dust of comet Halley was during the Giotto spacecraft flyby in 1986. Little of the refractory organics were lost in interplanetary space between the moment of ejection in 1767 and Earth impact in 2001.

This interpretation implies that a significant fraction of the hydrogen in the refractory organics is lost during ablation, possibly in a process known as carbonization that leads to the loss of functional groups and the formation of aromatic structures (*e.g.,* Jenniskens *et al.,* 1993).

Difficulties with the proposed interpretation of the origin of the H_α emission line remain. The Geminid meteor does not have detectable ionized silicon emission, which makes it remarkable that the hydrogen line is clearly detected. The Si II line has an upper energy state of 10.07 eV, lower than the 12.09 eV of H_α. If the line is merely weak, then the corresponding [C]/[Si] ratio would be significantly higher than that of the Leonid. Of course, the Geminid meteor also had stronger iron lines than calcium emissions, which leaves open the possibility that not all of the silicon is evaporated. Alternatively, a smaller fraction of silicon could be in the ionized state in a Geminid meteor, not consistent with T = 10,000 K.

There is also the more fundamental question as to whether such a hot component exists. Borovička (1994a) assigned the O I and N I lines to hot plasma because these lines originate from high excitation levels. In contrast, the N_2 First Positive band was assigned to the warm 4,400 K component, despite its high excitation energy. Since that time, we have demonstrated that all meteoric air plasma emissions match well to laboratory air plasma in local thermodynamic equilibrium at T = 4,400 K (Jenniskens *et al.,* 2000a, 2004b).

CONCLUSIONS

The H_α line was identified in the meteor spectra of three meteoroids originating from three different comets. The intensity of the high-excitation hydrogen emission followed the high-excitation N I and N_2 air plasma emissions, not the intensity of the low-excitation calcium, iron, and sodium lines in the meteor afterglow.

Nearly independent of the adopted excitation temperature, we calculated from the H/N line intensity ratio that if that hydrogen originated in the ambient atmosphere, then the hydrogen atom abundance at the altitude of the Leonid meteor (80–90 km) would have been in excess of 150 ± 20 ppm, a factor of about 11 ± 4 above the expected abundance of hydrogen in the form of H I, H_2, and H_2O. The evaporation and dissociation of water clusters and small ice particles are probably too slow to account for the difference.

On the other hand, if the hydrogen originated from a high excitation temperature $T \sim$10,000 K plasma component, perhaps from non-thermal collisions in the expansion phase of the meteor, and Si II emission originated from that same process, then it is possible that all of the observed hydrogen emission originated from hydrogen

atoms ablated from the meteoroid. We measured a hydrogen abundance for the Leonid meteoroid of comet 55P/Tempel-Tuttle within a factor of 2 from that measured in the dust of comet 1P/Halley during the 1986 flyby.

Unless there was 10 times more water vapor in the upper atmosphere than expected, all of the observed hydrogen in meteor spectra can have originated from the meteoroid, either from ablating refractory organic matter or from water trapped and bound in minerals. If the hydrogen originated from the meteoric organic matter, then that organic matter lost a significant fraction of its hydrogen during ablation, perhaps in a process known as carbonization. This would imply that the refractory organic matter was not lost in the vacuum of space since the meteoroid was ejected by the comet in 1767.

ACKNOWLEDGMENTS

This paper benefited greatly from comments by referees Jiri Borovička (Ondrejov Observatory, Czech Republic) and Shinsuke Abe (ISAS, Japan). NASA Ames Astrobiology Academy student Emily Schaller operated the CCD spectrograph during the 2001 Leonid MAC mission. The instrument was developed with support of NASA Ames Research Center's Director's Discretionary Fund. We thank Mike Koop, Mike Wilson, and Gary Palmer for technical support. Mike Koop also supported the ground-based 2001 Geminid campaign. The 2001 Leonid MAC mission was sponsored by NASA's Astrobiology ASTID and Planetary Astronomy programs and executed by the USAF 418th Flight Test Squadron. Greg Schmidt was the technical monitor at NASA Ames Research Center. This work meets with objective 3.1 of NASA's Astrobiology Roadmap (Des Marais *et al.*, 2003).

ABBREVIATIONS

CCD, charge coupled device; H_α, hydrogen Balmer-alpha; MAC, Multi-Instrument Aircraft Campaign; UT, universal time.

REFERENCES

Abe, S., Yano, H., Ebizuka, N., Kasuga, T., Watanabe, J.-I., Sugimoto, M., Fujino, N., Fuse, T., and Ogasawara, R. (2002) First results of OH emission from meteor and after glow: Search for organics in cometary meteoroids. In *ESA SP-500: Proceedings of Asteroids, Comets, Meteors (ACM 2002)*, ESA Publications Division, Noordwijk, The Netherlands, pp. 213–216.

Borovička, J. (1993) A fireball spectrum analysis. *Astron. Astrophys.* 279, 627–645.

Borovička, J. (1994a) Two components in meteor spectra. *Planet. Space Sci.* 42, 145–150.

Borovička, J. (1994b) Line identification in a fireball spectrum. *Astron. Astrophys. Suppl. Ser.* 103, 83–96.

Borovička, J. and Jenniskens, P. (2000) Time resolved spectroscopy of a Leonid fireball afterglow. *Earth Moon Planets* 82-83, 399–428.

Brack, A. (1999) Life in the Solar System. *Adv. Space Res.* 24, 417–433.

Ceplecha, Z. (1971) Spectral data on terminal flare and wake of double-station meteor No. 38421 (Ondrejov, April 21, 1963). *Bull. Astron. Inst. Czech.* 22, 219–304.

Chyba, C.F. and Sagan, C. (1992) Endogenous production, exogenous delivery and impact shock synthesis of organic molecules: An inventory for the origins of life. *Nature* 355, 125–132.

Chyba, C.F. and Sagan, C. (1997) Comets as a source of prebiotic organic molecules for the early Earth. In *Comets and the Origin and Evolution of Life*, edited by P.J. Thomas, C.F. Chyba, and C.P. McKay, Springer Verlag, New York, pp. 147–173.

Conway, R.R., Stevens, M.H., Brown, C.M., Cardon, J.G., Zasadil, S.E., and Mount, G.H. (1999) The Middle Atmosphere High Resolution Spectrograph Investigation. *J. Geophys. Res.* 104, 16327–16348.

Cook, A.F. and Millman, P.M. (1955) Photometric analysis of a spectrogram of a Perseid meteor. *Astrophys. J.* 121, 250–270.

Delsemme, A.H. (1992) Cometary origin of carbon, nitrogen and water on the Earth. *Origins Life* 21, 279–298.

Des Marais, D.J., Allamandola, L.J., Benner, S.A., Deamer, D., Falkowski, P.G., Farmer, J.D., Hedges, S.B., Jakosky, B.M., Knoll, A.H., Liskowsky, D.R., Meadows, V.S., Meyer, M.A., Pilcher, C.B., Nealson, K.H., Spormann, A.M., Trent, J.D., Turner, W.W., Woolf, N.J., and Yorke, H.W. (2003) The NASA Astrobiology Roadmap. *Astrobiology* 3, 219–235.

Greenberg, J.M. (2000) From comets to meteors. *Earth Moon Planets* 82-83, 313–324.

Harris, M.J. (2001) A new coupled middle atmosphere and thermosphere general circulation model: Studies of dynamic, energetic and photochemical coupling in the middle and upper atmosphere [Ph.D. Thesis], Department of Physics and Astronomy, University College London, London.

Harvey, G.A. (1977) A search for ultraviolet OH emission from meteors. *Astrophys. J.* 217, 688–690.

Jenniskens, P. and Rairden, R.L. (2000) Buoyancy of the "Y2K" persistent train and the trajectory of the 04:00:29 UT Leonid fireball. *Earth Moon Planets* 82-83, 457–470.

Jenniskens, P. and Russell, R.W. (2003) The 2001 Leonid Multi-Instrument Aircraft Campaign—an early review. *ISAS SP* 15, 3–15.

Jenniskens, P. and Stenbaek-Nielsen, H.C. (2004) Meteor wake in high frame-rate images—implications for the chemistry of ablated organic compounds. *Astrobiology* 4, 95–108.

Jenniskens, P., Baratta, G.A., Kouchi, A., de Groot, M.S., Greenberg, J.M., and Strazzulla, G. (1993) Carbon dust formation on interstellar grains. *Astron. Astrophys.* 273, 583–600.

Jenniskens, P., Wilson, M.A., Packan, D., Laux, C.O., Boyd, I.D., Popova, O.P., and Fonda, M. (2000a) Meteors: A delivery mechanism of organic matter to the early Earth. *Earth Moon Planets* 82-83, 57–70.

Jenniskens, P., Lacey, M., Allan, B.J., Self, D.E., and Plane, J.M.C. (2000b) The dynamical evolution of a tubular Leonid persistent train. *Earth Moon Planets* 82-83, 471–488.

Jenniskens, P., Tedesco, E., Murthy, J., Laux, C.O., and Price S. (2002) Spaceborne ultraviolet 251–384 nm spectroscopy of a meteor during the 1997 Leonid shower. *Meteoritics Planet. Sci.* 37, 1071–1078.

Jenniskens, P., Schaller, E.L., Laux, C.O., Wilson, M.A., Schmidt, G., and Rairden, R.L. (2004a) Meteors do not break exogenous organic molecules into high yields of diatomics. *Astrobiology* 4, 67–79.

Jenniskens, P., Laux, C.O., Wilson, M.A., and Schaller, E.L. (2004b) The mass and speed dependence of meteor air plasma temperatures. *Astrobiology* 4, 81–94.

Jenniskens, P., Laux, C.O., and Schaller, E.L. (2004c) Search for the OH ($X^2\Pi$) Meinel band emission in meteors as a tracer of mineral water in comets: Detection of $N_2^+(A\text{-}X)$. *Astrobiology* 4, 109–121.

Kondrat'eva, E.D. and Reznikov, E.A. (1985) Comet Tempel-Tuttle and the Leonid meteor swarm. *Solar System Res.* 19, 96–101.

Lellouch, E., Crovisier, J., Lim, T., Bockelee-Morvan, D., Leech, K., Hanner, M. S., Altieri, B., Schmitt, B., Trotta, F., and Keller, H.U. (1998) Evidence for water ice and estimate of dust production rate in comet Hale-Bopp at 2.9 AU from the Sun. *Astron. Astrophys.* 339, L9–L12.

Maurette, M., Duprat, J., Engrand, C., Gounelle, M., Kurat, G., Matrajt, G., and Toppani, A. (2000) Accretion of neon, organics, CO_2, nitrogen and water from large interplanetary dust particles on the early Earth. *Planet. Space Sci.* 48, 1117–1137.

Millman, P. (1980) One hundred and fifteen years of meteor spectroscopy. In *Solid Particles in the Solar System,* edited by I. Halliday and B.A. McIntosh, D. Reidel Publishing Co., Dordrecht, The Netherlands, pp. 121–128.

Oró, J. (1961) Comets and the formation of biochemical compounds on the primitive Earth. *Nature* 190, 389–390.

Plane, J.M.C. (2000) The role of sodium bicarbonate in the nucleation of noctilucent clouds. *Ann. Geophys.* 18, 807–814.

Poole, L.M.G. (1979) The excitation of spectral lines in faint meteor trains. *J. Atmospheric Terr. Phys.* 41, 53–64.

Rietmeijer, F.J.M. and Nuth, J.A. (2000) Collected extraterrestrial materials: Constraints on meteor and fireball compositions. *Earth Moon Planets* 82-83, 325–350.

Roble, R. (1995) *Geophysical Monograph 87: Energetics of the Mesosphere and Thermosphere. Upper Mesosphere and Lower Thermosphere: A Review of Experiment and Theory,* American Geophysical Union, Washington, DC.

Stevens, M.H., Conway, R.R., Englert, C.R., Summers, M.E., Grossman, K.U., and Gusev, O.A. (2001) PMCs and the water frost point in the Arctic summer mesosphere. *Geophys. Res. Lett.* 28, 4449–4452.

Address reprint requests to:
Dr. Peter Jenniskens
Center for the Study of Life in the Universe
SETI Institute
2035 Landings Drive
Mountain View, CA 94043

E-mail: pjenniskens@mail.arc.nasa.gov